

Mechanistic Study of Macranthoside B Effects on Apoptotic Cell Death in Human Cervical Adenocarcinoma Cells

(macranthoside B / oxidative stress / Akt/PDK1 / antioxidant enzymes / apoptosis)

Y. LI¹, M. LI^{2,3}, K. AHMED⁴, J. YANG¹, L. SONG¹, Z. G. CUI³, Y. HIRAKU³

¹School of Life Science and Technology, Henan Institute of Science and Technology, Xinxiang, China

²School of Medicine, Xizang Minzu University, Weicheng District, Xianyang, Shaanxi, China

³Department of Environmental Health, University of Fukui School of Medical Sciences, Fukui, Japan

⁴Faculty of Eastern Medicine, Hamdard University, Islamabad, Pakistan

Abstract. Macranthoside B (MB) is a triterpenoid saponin extracted from *Lonicera macranthoides*, a traditional Chinese medicine. In the current study, we investigated the anticancer potential of MB in various cancer cells and elucidated its underlying mechanisms. MB exposure inhibited cell proliferation, induced mitochondrial membrane potential (MMP) loss, increased sub-G1 accumulation, and resulted in cleavage of caspase-3 and PARP, which are reflective of apoptosis. In HeLa cells, MB induced down-regulation of SOD2 and GPx1, phosphorylation of Akt and PDK1, and thus promoted ROS-mediated apoptosis. This was further supported by the protection of sub-G1 accumulation, MMP loss, cleavage of caspase-3 and PARP in the presence of N-acetylcysteine (NAC). Additionally, MB induced cell death via

down-regulation of ubiquitin-like with PHD and ring-finger domains 1 (UHRF1) and Bcl-xL. Taken together, this study provides a new insight into the apoptosis-inducing potential of MB, and its molecular mechanisms are associated with an increase in oxidative stress and inhibition of the PDK1/Akt pathway.

Introduction

Cancer is the second leading cause of death in humans globally. Every year more than 7 million deaths are reported due to cancer (Prasedya et al., 2016). Among women, cervical cancer has been reported to cause high morbidity and mortality, with only 66 % of the 5-year survival rate reported in developing countries (Ferlay et al., 2015). Despite treatment options of surgery, radiotherapy and chemotherapy, the survival rate in patients with cervical cancer remains low due to metastasis, radio-resistance and drug resistance (Bhatla et al., 2018). To particularly address these problems, a continuous search for chemicals or naturally occurring compounds that are of therapeutic value is needed to improve the odds of survival for patients with cervical cancer.

Natural plants could be considered reservoirs of novel chemical entities, from which some extracts were able to produce chemical compounds that have emerged as prospective anticancer agents potentially offering promising outcomes. For example, natural bioactive products of flavonoids, terpenoids and saponins have been reported to possess potential anticancer activity (Avato et al., 2017; Joshi et al., 2017; Majumder et al., 2017). An extract from *Lonicera macranthoides*, macranthoside B (MB) (Fig. 1A), is a triterpenoid saponin that has been traditionally used in Chinese medicine for many diseases including cancer (Chen et al., 2009; Wang et al., 2009; Guan et al., 2011). It has also been reported that saponins have protective effects on hepatic injury caused by acetaminophen and chemokine (C-C motif) ligand 4 (CCl₄)-induced hepatic injury (Ohta et al., 1993; Jiang et al., 2014). MB has also been reported

Received October 25, 2021. Accepted February 20, 2023.

This study was supported by Key technologies R&D program of Henan Province (grant No. 202102110166), Key R&D special projects of Henan Province (grant No. 221111110300) and Key scientific and technological projects in Henan Province (grant No. 212102310876).

Corresponding authors: Zheng-Guo Cui, Department of Environmental Health, University of Fukui School of Medical Sciences, 23-3, Matsuokashimoaizuki, Eiheiji-cho, Yoshida-gun, Fukui, 910-1193, Japan. Phone: +81 776 61 8337; Fax: +81 776 61 8107; e-mail: sai@u-fukui.ac.jp. Yusuke Hiraku, Department of Environmental Health, University of Fukui School of Medical Sciences, 23-3, Matsuokashimoaizuki, Eiheiji-cho, Yoshida-gun, Fukui, 910-1193, Japan. Phone: +81 776 61 8335; Fax: +81 776 61 8107; e-mail: y-hiraku@u-fukui.ac.jp

Abbreviations: MB – macranthoside B, MMP – mitochondrial (trans)membrane potential, NAC – N-acetylcysteine, PARP – poly-ADP ribose polymerase, PBS – phosphate-buffered saline, PDK1 – pyruvate dehydrogenase kinase 1, ROS – reactive oxygen species, UHRF1 – ubiquitin-like with PHD and ring-finger domains 1.

to induce reactive oxygen species (ROS)-mediated apoptosis in human ovarian cancer A2780 cells and human promyelocytic leukaemia HL-60 cells; however, the detailed underlying mechanisms still remain unclear (Wang et al., 2009; Guan et al., 2011).

The phosphoinositol-3-kinase (PI3K)-Akt pathway is a representative anti-apoptotic effector promoting invasion and metastasis (Lazorchak and Su, 2011; Wang et al., 2019). Over-expression and dysregulation of the PI3K-Akt pathway associated with cell death have been reported frequently in various types of cancer (Nitulescu et al., 2018). Phosphorylation of second messenger phosphatidylinositol-4,5-bisphosphate (PIP2) to phosphatidylinositol-3,4,5-triphosphate (PIP3) is the main function of PI3Ks. PIP3 can bind to both phosphoinositide-dependent kinase 1 (PDK1) and Akt protein, and recruits the Akt protein at the plasma membrane. Plasma membrane-bound PDK1 is able to phosphorylate and activate Akt (Choi et al., 2008). Persistent activation of Akt is responsible for cancer cell survival and excessive proliferation through the inhibition of apoptotic processes. Over-expression of Akt is notably associated with the progression of cervical cancer (Prasad et al., 2015; Bahrami et al., 2017). Therefore, the PI3K/Akt signalling pathway represents a valuable target for the exploration of new pharmacological agents against cervical cancer.

The current study was undertaken to evaluate the effects of MB targeting the PI3K-Akt signalling pathway and the subsequent effects on the cell proliferation and apoptosis induction in human cervical adenocarcinoma, HeLa cells. ROS play important roles in cell death by modification of various physiological and pathological signal transduction mechanisms including the PI3K-Akt pathway. We also examined the changes in intracellular ROS generation, the expression levels of antioxidant enzymes, and the associated anti-apoptotic proteins such as ubiquitin-like with PHD and ring-finger protein 1 (UHRF1) and Bcl-xL.

Material and Methods

Reagents, cell culture and treatment

MB was purchased from Chengdu Herb Purify Co., LTD., Sichuan Prov., China. Cervical adenocarcinoma HeLa, mammary epithelial adenocarcinoma MCF7, and epithelial glioblastoma U87 (or U-87 MG), epithelial-like lung cancer A549, and hepatocellular carcinoma HepG2 cell lines were obtained from the Human Science Research Resources Bank Japan (Japan Human Sciences Foundation, Tokyo, Japan). The cells were cultured and maintained in low-glucose Dulbecco's Modified Eagle's Medium supplemented with 10 % heat-inactivated foetal bovine serum (FBS; Thermo Scientific, Waltham, MA) in a humidified incubator at 37 °C with 5 % CO₂ and 95 % air, and the medium was changed every other day. The cells were harvested by trypsinization with 0.05 % cold trypsin and sub-cultured according to the

specific experimental requirements. The cells were allowed to adhere to the bottom of the dish for 24 h after seeding, and the growth medium was changed with a freshly prepared medium before treatment.

Cell viability analysis by MTT assay

Cell viability was assessed by the MTT [(3-(4,5-dimethyl-2-thiazolyl)-2,5-diphenyl-2-H-tetrazolium bromide) assay. The cells were cultured in 96-well plates at a density of 5×10^3 cells/well and incubated overnight to allow for surface attachment before the 24 h treatment with the indicated concentrations of MB. Next, the MTT solution (5 mg/ml, 10 µl/well) was added to the 96-well plates and incubated for 3 h at 37 °C. Afterwards, the medium containing MTT was removed and replaced with 150 µl/well dimethyl sulphoxide (DMSO). The plates were then subjected to constant shaking for 5 min to solubilize the formazan crystals. The absorbance of the solution at 540 nm was measured with a microplate reader according to a method reported previously (Yun et al., 2016). This assay was conducted in triplicate, and the cell viability was calculated as a percentage of viable cells in the drug-treated group versus the non-treated (NT) control group using the following equation: cell viability (%) = [OD (drug treatment) – OD (blank)]/[OD (control) – OD (blank)] × 100.

Sub-G1 analysis

Cell cycle analysis was performed following a protocol reported previously (Riccardi and Nicoletti, 2006). Briefly, after collection, cells were washed with phosphate-buffered saline (PBS) followed by centrifugation at 400 g for 5 min at 4 °C and resuspension in 50 µl of PBS after the drop-by-drop addition of 70 % ice-cold ethanol. The fixed cells were stored at –20 °C for at least 2 h, rehydrated with PBS, and staining was done with propidium iodide (PI) solution containing RNase for 30 min at room temperature. The cell cycle phases were analysed using a flow cytometer (BD FACSCanto II Flow Cytometer ver. 1.1 and Diva 6.1, BD Biosciences, Franklin Lakes, NJ). A minimum of 10,000 cells per sample was evaluated at a flow speed of fewer than 400 cells/s, and the cell debris was excluded from the analysis. The cells with decreased DNA staining (hypodiploid cells) in the sub-G1 phase were considered as apoptotic cells. The data were analysed using Flowing Software 2.5.1 (Turku Bioscience, Turku, Finland).

Western blotting

Western blot analysis was carried out according to the method described previously (Cui et al., 2006). Briefly, cells were collected and after washing with PBS, lysed for 20 min on ice with RIPA buffer which contains 150 mM NaCl, 1 % Triton X-100 (v/v), 1 % sodium deoxycholate, 0.1 % SDS, 1 µg/ml each protease inhibitor (aprotinin, pepstatin and leupeptin), 1 mM EGTA, 50 mM Tris-HCl, pH 7.5. After a brief sonication, the lysates were centrifuged at $13,000 \times g$ for 10 min at 4 °C, and the protein content in the supernatant was measured by

using a Coomassie (Bradford) Protein Assay Kit (Thermo Scientific, Waltham, MA). The protein lysates were mixed with SDS loading buffer, denatured at 96 °C for 10 min, separated by SDS-polyacrylamide gel electrophoresis and transferred to a nitrocellulose membrane (Amersham Biosciences, Buckinghamshire, UK) (Sambrook et al., 1989). Afterwards, the membrane was blocked with 5 % skim milk in TBST (150 mM NaCl, 50 mM Tris, pH 7.5, 0.1 % Tween-20). Western blot analysis was performed using the following specific monoclonal or polyclonal antibodies: anti-cleaved PARP, anti-cleaved caspase-3, anti-Bcl-xL, anti-superoxide dismutase-2 (SOD2), anti-glutathione peroxidase-1 (GPx1), anti-p-AKT^{Ser473}, anti-AKT (pan), anti-p-PDK1^{Ser241}, anti-UHRF1 and anti- β -actin (Santa Cruz Biotechnology, Inc., Dallas, TX) antibodies. Blots were then probed with secondary horseradish peroxidase (HRP)-conjugated anti-rabbit or anti-mouse IgG antibodies (Cell Signaling Technology, Inc., Danvers, MA). For the detection of proteins, chemiluminescence agents ECL and ECL Ultra were used according to the manufacturer's instructions (Amersham Biosciences, Amersham, UK), and band signals were visualized by using a luminescent image analyser (LAS4000, Fujifilm Co., Tokyo, Japan). Densitometric analysis of protein expression was performed by using Image Studio Digits ver. 5.0 (LI-COR Biosciences, Lincoln, NE), and the values were normalized to those of β -actin.

Detection of mitochondrial membrane potential (MMP)

After collection, the cells were washed and stained with 10 nM tetramethylrhodamine, methyl ester, perchlorate (TMRM) in 1 ml of 1 × PBS for 15 min at 37 °C following the method developed by Zakki et al. (2018). The percentage of cells with a low MMP was detected by flow cytometry (BD FACSCanto II Flow Cytometer ver. 1.1 and Diva 6.1), and data were analysed using Flowing Software 2.5.1 (Turku Bioscience).

Measurement of ROS generation

ROS levels were assessed by utilizing molecular probe dihydroethidine (DHE). DHE is oxidized by superoxide anion (O_2^-) within the cell to produce ethidium bromide, which fluoresces when it intercalates into DNA (Johnson-Cadwell et al., 2007). The fluorescence emission was then analysed by a flow cytometer following the previously published method (Li et al., 2019). Briefly, after collection, the cells were incubated separately for 30 min at 37 °C with 1 μ g/ml DHE. After washing twice with PBS, the stained cells were measured using a flow cytometer (BD FACSCanto II Flow Cytometer ver. 1.1 and Diva 6.1), and the result was analysed by using Flowing Software 2.5.1 (Turku Bioscience).

Statistical analysis

All experiments were performed in at least three independent replicates. Data are presented as the mean \pm standard error. All statistical analyses were done by using version 6.0 of GraphPad Prism (GraphPad Prism Software, San Diego, CA). One-way analysis of variance (ANOVA) with Tukey's multiple comparison tests were performed for cell viability assay, sub-G1 fractions, ROS and fractions of low MMP, whereas two-way ANOVA with Bonferroni post tests for group experiments were performed for the measurement of relative ratios of protein expression. P values < 0.05 were considered as statistically significant.

Results

MB decreased cell viability of HeLa cells

To investigate the effect of MB treatment on the viability of HeLa cells, the MTT assay was performed. Cells were treated with MB at different concentrations for 24 h. As shown in Fig. 1B, addition of 20 μ M MB decreased the viability of HeLa cells to 85.3 % (P <

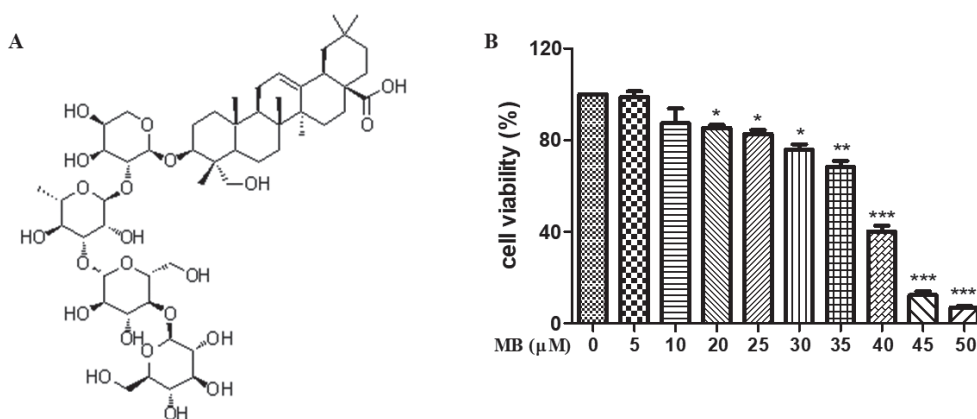


Fig. 1. Macranthoside B (MB) decreased cell viability in HeLa cells. **A:** Chemical structure of MB. **B:** HeLa cells were treated with the indicated concentrations of MB for 24 h, and cell viability was evaluated using the MTT assay. The data in each bar graph are presented as the means \pm SEM. (N = 3). *P < 0.05, **P < 0.01 and ***P < 0.001 relative to control.

0.05) compared to the control cells. At the higher concentrations (25 μ M, 30 μ M, 35 μ M, 40 μ M, 45 μ M and 50 μ M) of MB treatment, further reduction in viability of HeLa cells to 82.7 % ($P < 0.05$), 75.8 % ($P < 0.05$), 68.3 % ($P < 0.01$), 40.1 % ($P < 0.001$), 12.3 % ($P < 0.001$) and 6.9 % ($P < 0.001$), respectively, was observed. The result of the cell viability assay suggests that MB significantly reduces the proliferation of HeLa cells in a concentration-dependent manner.

MB induced apoptosis in HeLa cells

To examine the mechanism behind the anti-proliferative activity of MB, cells were analysed based on their growth cycle stages by flow cytometry. As shown in Fig. 2A and B, MB induced a slight and significant increase in sub-diploid DNA, a characteristic of apoptotic cells that are accumulated in the sub-G1 position of the cell cycle, at 35 μ M and a marked increase was observed

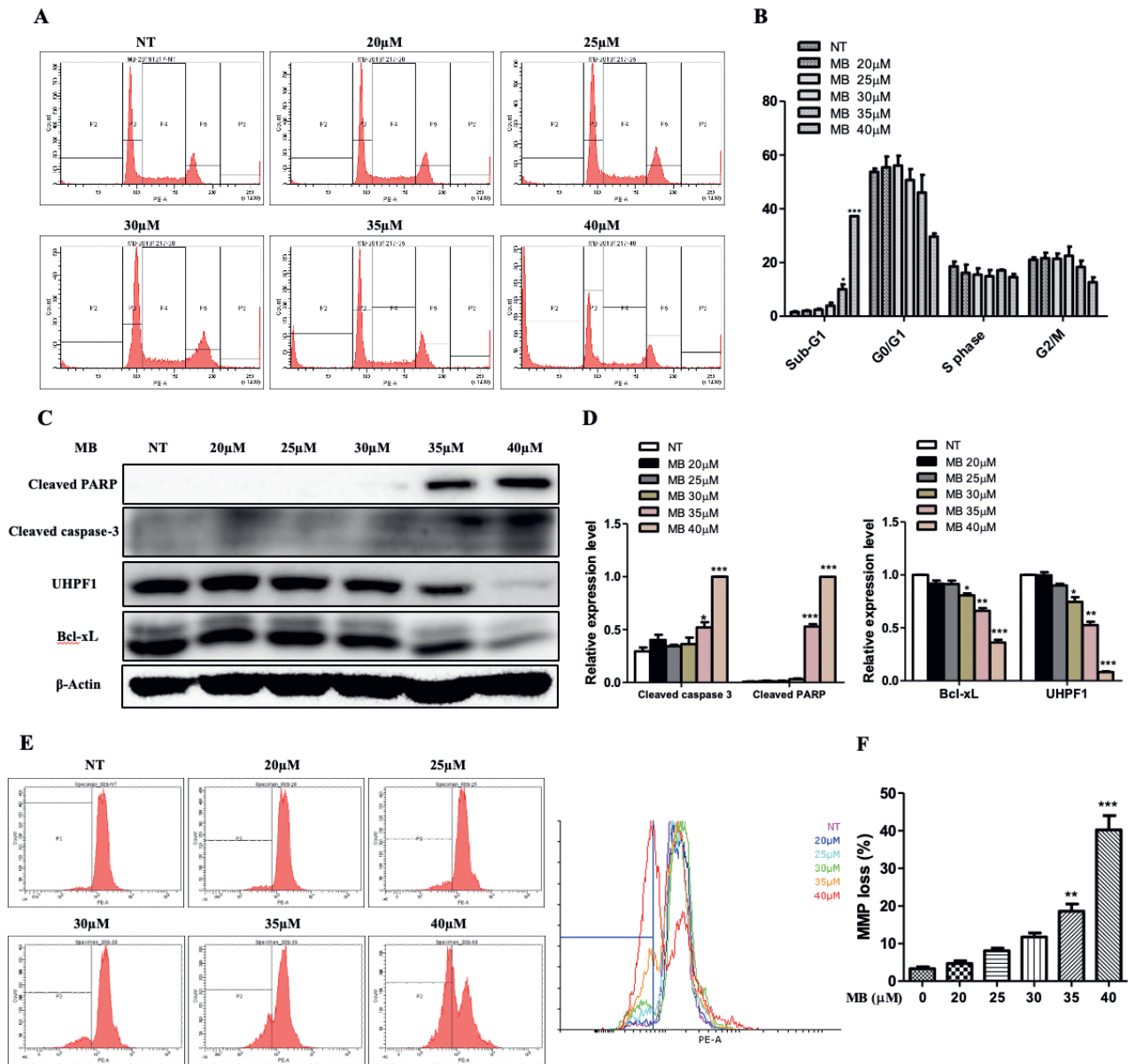


Fig. 2. MB induced apoptosis in HeLa cells. **A:** Sub-G1 phase accumulation was evaluated by flow cytometry; **B:** analysis of the cell population at each cell cycle phase relative to total phases. **C:** The levels of pro- and anti-apoptotic proteins were further analysed by Western blotting. **D:** Quantification of the proteins was performed. β -Actin was used as an internal loading control. **E:** Overlay histogram representing MMP loss with the formation of left-side waves indicates loss of potential, compared with the right-side wave showing high potential in control and healthy cells. The Y-axis shows the number of cells. The X-axis shows the potential of the mitochondrial membrane. **F:** Fraction of cells with a low MMP (%). The data are presented in each bar graph as the means \pm SEM. (N = 3). * $P < 0.05$, ** $P < 0.01$ and *** $P < 0.001$ relative to control.

at 40 μM . To further investigate the apoptotic mechanism of MB in HeLa cells, we examined the expression levels of certain anti- and pro-apoptotic proteins by Western blotting. As shown in Fig. 2C and D, cleavage of poly (ADP-ribose) polymerase (PARP) and caspase-3 was markedly increased at 35 and 40 μM , whereas anti-apoptotic proteins Bcl-xL and UHRF1 were significant-

ly decreased in a concentration-dependent manner. To check whether the mitochondrial pathway is involved in MB-induced apoptosis in HeLa cells, MMP was examined. As shown in Fig. 2E and F, a significant MMP loss was observed after MB treatment. This result suggests that MB could induce mitochondria-related apoptosis in HeLa cells.

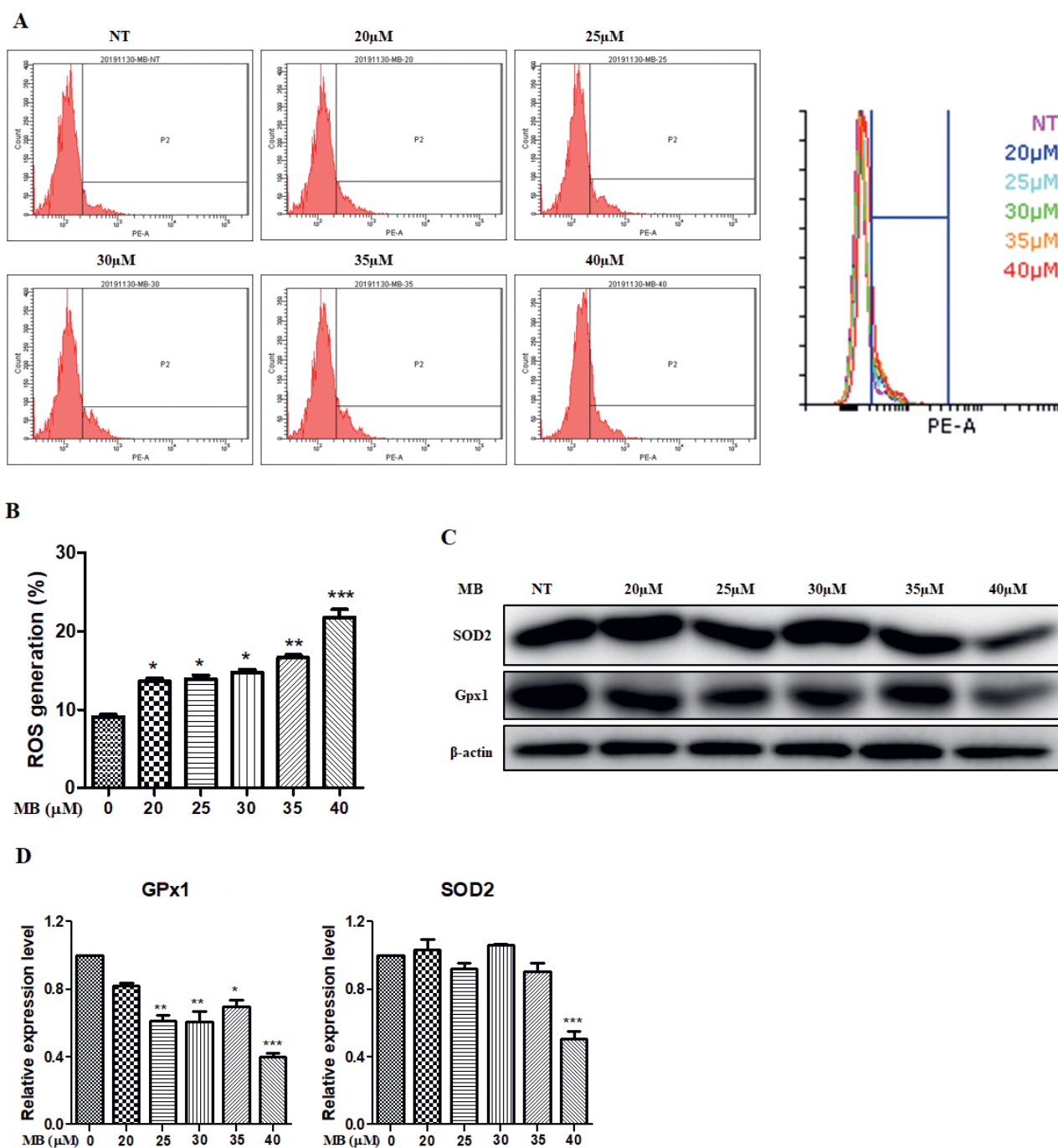


Fig. 3. MB increased ROS generation in HeLa cells. **A, B**: The levels of superoxide anions were analysed for ROS generation by flow cytometry using dihydroethidine (DHE) as a fluorescent probe. **C**: The levels of antioxidant proteins (GPx1 and SOD2) were measured by Western blotting. **D**: The relative expression levels of proteins were quantified by densitometric analysis. For internal loading control, β -actin was utilized. The data are presented in each bar graph as the means \pm SEM. (N = 3). * $P < 0.05$, ** $P < 0.01$ and *** $P < 0.001$ relative to control.

MB induced ROS generation in HeLa cells

ROS play an important role in apoptosis and are closely associated with mitochondria (Fonseca-Silva et al., 2011). It has been reported that accumulation of ROS may be responsible for mitochondrial dysfunction (Harris, 2003). Therefore, the generation of ROS was examined after treatment of HeLa cells with MB for 6 h. As presented in Fig. 3A and B, a significant increase in O_2^- generation was observed in a concentration-dependent manner. Cells tend to protect themselves from oxidative stress with the help of the antioxidant defence system. In this mechanism, O_2^- is converted into hydrogen peroxide (H_2O_2) with the assistance of SODs, whereas H_2O_2 is converted into water with the help of GPx and catalase. Consequently, with this defence system, two toxic species, O_2^- and H_2O_2 , are converted into harmless product water. Thus, to confirm the involvement of the antioxidant system, we analysed the expression levels of SOD2 and GPx1, and found them to be suppressed after MB treatment (Fig. 3C and D). These results indicate that the increase of oxidative stress is associated with MB-mediated apoptosis by inhibiting the antioxidant defence system in HeLa cells.

MB induced inhibition of Akt and PDK1 phosphorylation in HeLa cells

PKD1 and Akt (also known as protein kinase B) are pivotal enzymes in the cell survival pathway and are considered as primary targets when investigating the anticancer potential of a drug (Cragg and Newman, 2005). Therefore, we examined the effects of MB on phosphorylation of PKD1 and Akt at Ser473. As shown in Fig. 4A and B, MB significantly inhibited the phosphorylation of PDK1 and Akt. These findings indicate that inactivation of PDK1 and Akt at Ser473 plays a crucial role in the inhibition of cell proliferation and induction of apoptosis induced by MB.

Role of ROS in MB-induced cell growth inhibition and apoptosis events

To further explore the important role of ROS in MB-mediated effects on HeLa cells, we examined the effects of N-acetylcysteine (NAC), a ROS scavenger, on ROS generation and antioxidant enzymes SOD2 and GPx1. We pre-treated HeLa cells with 2 mM of NAC for 1 h followed by 40 μ M MB treatment for 6 h and examined ROS generation. As shown in Fig. 5A and B, NAC pre-treatment significantly prevented MB-induced O_2^- generation and recovered the expression of antioxidant proteins SOD2 and GPx1, as demonstrated in Fig. 5C and D. These results suggest that NAC prevents MB-induced oxidative stress in HeLa cells.

We then examined whether oxidative stress had any role in the cell proliferation and apoptosis events induced by MB. To check cell viability, we pre-treated HeLa cells with 2 mM of NAC for 1 h followed by 40 μ M MB treatment for 24 h. As shown in Fig. 6A, pre-treatment with NAC prevented any decrease in cell viability caused by MB. Furthermore, NAC pre-treatment also prevented MB-induced accumulation of cells in the sub-G1 phase (Fig. 6B and C). In addition, the results showed that NAC pre-exposure significantly prevented MB-induced MMP loss (Fig. 6D and E). In Fig. 6F and G, we further demonstrated that NAC significantly prevented MB-induced cleavage of PARP and caspase-3. These results suggest that oxidative stress plays an important role in MB-mediated apoptosis.

In addition, we investigated the effects of NAC on MB-mediated inactivation of the PDK1/Akt pathway. As shown in Fig. 7A and B, NAC pre-treatment significantly recovered the level of PDK1 and Akt phosphorylation inhibited by MB. These results confirm that MB-mediated oxidative stress is responsible for MB-induced inhibition of the PDK1/Akt pathway.

Finally, the cancer cell-killing effect of MB was also confirmed in various cancer cell lines. We treated MCF7

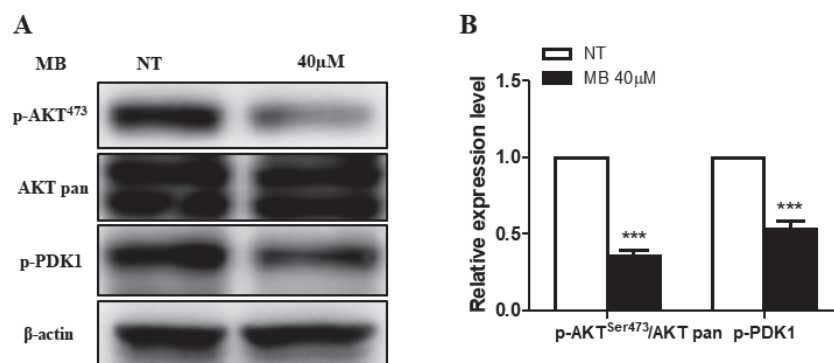


Fig. 4. MB dysregulated the Akt pathway in HeLa cells. **A:** The levels of Akt pathway components (p-Akt and PDK1) were measured by Western blotting. **B:** The relative expression levels of proteins were quantified by densitometric analysis. β -Actin was used as an internal loading control. The data are presented in each bar graph as the means \pm SEM. (N = 3). ***P < 0.001 relative to control.

(breast adenocarcinoma), U87 (epithelial glioblastoma), A549 (epithelial lung cancer), and HepG2 (hepatocellular carcinoma) cells with MB for 24 h. Importantly, as with HeLa cells, MB treatment significantly suppressed viability and MMP, dramatically induced apoptotic cell death (Fig. 8A–D), further confirming the anticancer effects of MB.

Discussion

Natural bio-products are important sources of pharmaceutical agents. With the aim of developing novel chemotherapeutic agents for cancer therapy, several ongoing studies investigate natural plant components for potential anticancer activities (Bagli et al., 2004; Nitulescu et al., 2016). It has been reported that the top 20 of the marketed drugs today were discovered from different natural resources, a finding that underscores the importance of developing anticancer agents from natural medicine (Sun et al., 2011; Redza-Dutordoir and Averill-Bates, 2016).

MB, a triterpenoid saponin extracted from *Lonicera macranthoides*, has not been extensively studied for its anticancer activities. To our knowledge, this is the first

study to report on the potential anticancer effects of MB in cervical cancer HeLa cells by targeting the PI3K/Akt signalling pathway. In this study, we demonstrated that the viability of HeLa and other cancer cell lines was significantly decreased after 24 h exposure to MB in a dose-dependent manner. Moreover, it induced accumulation of cells in the sub-G1 phase, reflecting apoptotic cell death (Fig. 2A and Fig. 8). Cleavage of caspase-3 and PARP are key events in the process of apoptosis. After MB treatment, we found prominent cleavage of caspase-3, which resulted in the cleavage of PARP (Fig. 2C and D). It further indicates the potential effects of MB on the induction of apoptotic cell death in HeLa cells.

The PI3K-Akt signalling pathway regulates essential cellular survival, proliferation, and migration. Activation of PI3K results in the recruitment of PDK1 and Akt to the plasma membrane (Bagli et al., 2004). Abnormal activation of Akt promotes cancer cell proliferation, survival, and resistance against cancer therapy. The overexpression and activation of Akt have been shown to be responsible for the resistance to chemotherapy or radiotherapy by certain types of cancers (Nitulescu et al., 2016). Therefore, targeting PI3K/Akt is considered a

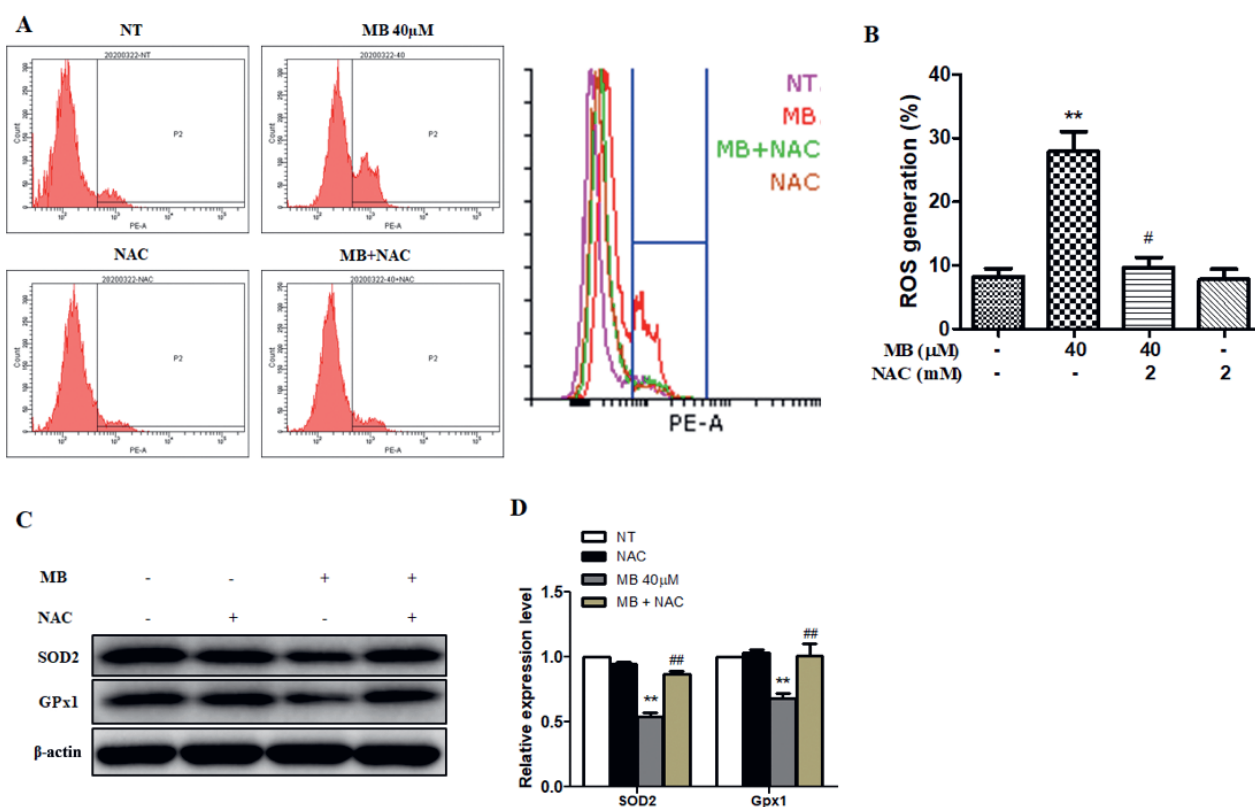


Fig. 5. NAC inhibited ROS generation induced by MB in HeLa cells. **A, B**: Cells were pre-treated with 2 mM NAC for 1 h followed by 40 μ M MB for 6 h. The levels of ROS are presented as fractions of cells with high ROS in HeLa cells. DHE was used as a fluorescent probe. **C**: The levels of antioxidant proteins (GPx1 and SOD2) were measured by Western blotting after 24 h MB exposure. **D**: The relative expression levels of proteins were quantified by densitometric analysis. β -Actin was used as an internal loading control. The data are presented in each bar graph as the means \pm SEM. (N = 3). **P < 0.01 relative to control. #P < 0.05, ##P < 0.01 relative to MB treatment.

well-grounded strategy for anticancer drug discovery. Previously, it has been reported that Chinese herbal medicine luteolin, a common flavonoid, exerts its anticancer activity by suppressing activation of the Akt kinase (Redza-Dutordoir and Averill-Bates, 2016). In our study, MB also showed significant anti-proliferative activity via suppression of Akt and PDK1 phosphorylation

(Fig. 4A and B). In addition, NAC pre-exposure prevented the MB-induced inactivation of Akt and PDK1 (Fig. 7A and B), suggesting the important contribution of oxidative stress and PI3K-Akt pathway in the anti-proliferative action of MB in HeLa cells.

To further unfold details of the mechanism behind the MB-induced effects, we investigated the roles of anti-

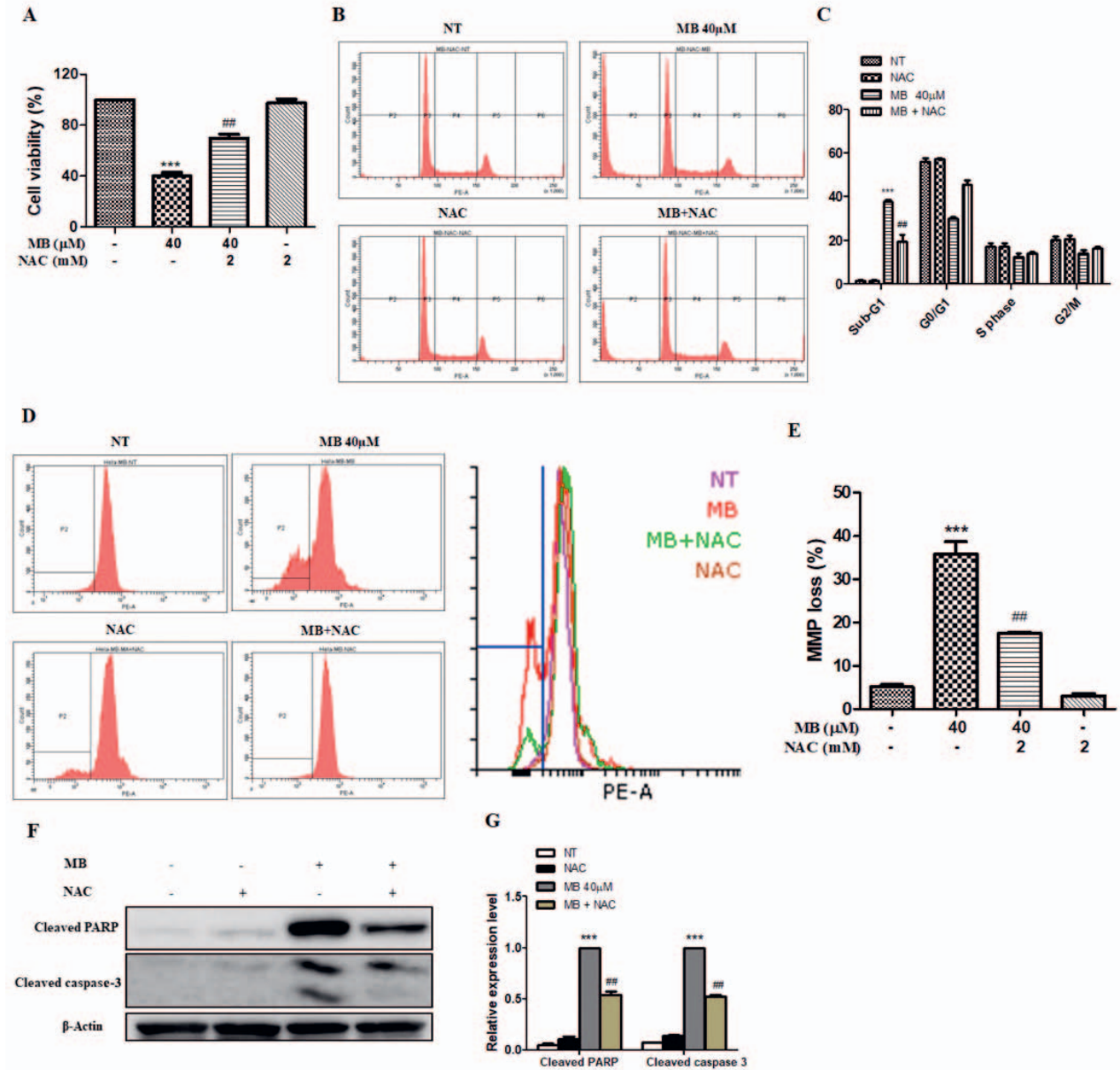


Fig. 6. ROS scavenger NAC inhibited the cytotoxicity of MB in HeLa cells. Cells were pre-treated with NAC for 1 h followed by 24 h MB treatment. **A**: Cell viability was evaluated using the MTT assay. **B**: Sub-G1 phase accumulation was evaluated by flow cytometry. **C**: Analysis of the cell population at each cell cycle phase relative to total phases. **D**: Overlay histogram representing MMP loss detected by TMRM staining using flow cytometry (MB + NAC : co-treatment of MB and NAC). **E**: Fraction of cells with a low MMP (%). **F**: The protective effects of NAC against MB-induced apoptosis including caspase-3 and/or PARP cleavage were determined by Western blotting. **G**: The relative expression levels of proteins were quantified by densitometric analysis. β-Actin was used as an internal loading control. The data are presented in each bar graph as the means ± SEM. (N = 3). ***P < 0.001 relative to control. #P < 0.05 and ##P < 0.01 relative to MB treatment.

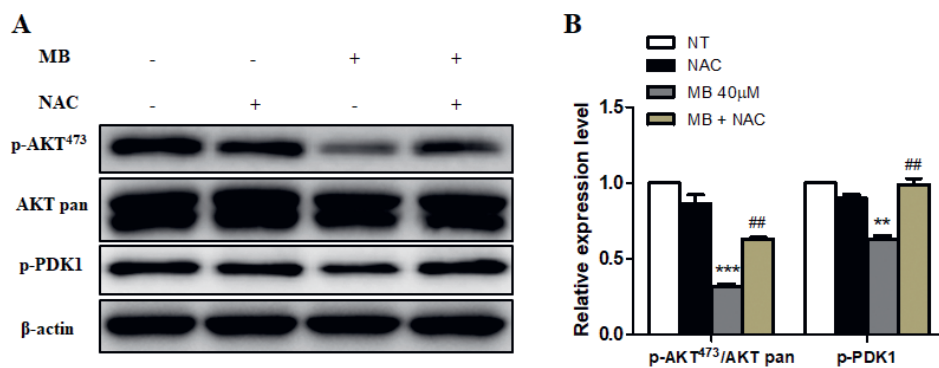


Fig. 7. NAC activated Akt in HeLa cells. Cells were pre-treated with NAC for 1 h followed by 24 h MB treatment. **A:** The levels of Akt pathway components (p-Akt and PDK1) were measured by Western blotting, and **B:** the relative expression levels of proteins were quantified by densitometric analysis. β -Actin was used as an internal loading control. The data are presented in each bar graph as the means \pm SEM. (N = 3). **P < 0.01 and ***P < 0.001 relative to control. ##P < 0.01 relative to MB treatment.

apoptotic proteins UHRF1 and Bcl-xL. UHRF1 is a putative oncogene over-expressed in various human malignancies, and up-regulation of UHRF1 helps the cancer cells to proliferate (Sun et al., 2011). It is over-expressed in cervical cancer and is reported to inhibit apoptosis, and reduces the radio-sensitivity of cervical cancer (Li et al., 2009). Up-regulation of UHRF1 is also reported to increase activity within the PI3K-Akt signalling pathway (Chen et al., 2019). Thus, inhibiting UHRF1 expression would be an efficient way to prevent the development of cervical cancer by blocking cell proliferation (Stevens and Oltean, 2019). Bcl-xL exerts potent anti-apoptotic roles by protecting release of cytochrome c from mitochondria (Webster, 2012). Interestingly, we demonstrated that MB significantly inhibited cell proliferation via down-regulation of UHRF1 and Bcl-xL expression (Fig. 2C and D).

The loss of MMP triggers the mitochondria-mediated apoptotic pathway. Following the loss of MMP, cytochrome c, which is localized in the intermembrane space and on the surface of the inner mitochondrial membrane, is released into the cytoplasm (Kharbanda et al., 1997) and interacts with apoptotic protease-activating factor 1 (Apaf-1) to form the apoptosome, which in turn activates caspase-9 and then caspase-3 and destroys PARP. Localized on the mitochondrial membrane, Bcl-xL is reported to prevent the MMP loss and cytochrome c release into the cytoplasm. As mentioned above, MB induces down-regulation of Bcl-xL (Fig. 2C and D), and our results also showed an increase in MMP loss (Fig. 2E and F) and cleavage of caspase-3 and PARP (Fig. 2C and D) in MB-treated HeLa cells, indicating that MB can induce apoptosis through a mitochondria- and caspase-dependent pathway in HeLa cells.

Changes in MMP also result in the generation of ROS, which trigger induction of apoptosis (Redza-Du-tordoir and Averill-Bates, 2016). In normal cells, with

the assistance of antioxidant defence systems such as SOD2, catalase, peroxiredoxins, glutathione and GPx, ROS exist in an equilibrium state. An increase of ROS leading to oxidative stress promotes cell death by oxidation of proteins, nucleic acids and lipids (Liu et al., 2009). It has been reported previously that MB induces ROS-mediated apoptosis in A2780 cells (Shan et al., 2016). In this study, MB significantly increased the O_2^- level (Fig. 3B), which contributed to cell death evidenced by prevention of accumulation of cells in the sub-G1 phase (Fig. 6B and C) and inhibition of cleavage of caspase-3 and PARP proteins in the presence of antioxidant NAC (Fig. 5F and G). The increase in ROS led us to investigate the effect of MB on antioxidant enzymes SOD2 and GPx1. It was discovered that MB decreased SOD2 and GPx1 expression (Fig. 3C). These results showed that MB induced oxidative stress by inducing ROS overproduction and reducing expression of antioxidants.

In conclusion, the present study has revealed that MB inhibits proliferation and induces apoptotic cell death of HeLa cells. Similar effects were also observed using MCF7, U87, A549 and HepG2 cancer cell lines (Fig. 8). The underlying molecular mechanisms were associated with an increase in oxidative stress and suppression of PDK1/Akt pathway, as well as anti-apoptotic proteins Bcl-xL and UHRF1 (Fig. 9). Thus, MB can now be considered as a new potential candidate chemotherapeutic agent that targets the PI3K/Akt signalling pathway in cancer cells. More studies will be needed to unravel additional details of the mechanism involved and to further explore the effect of MB anti-tumour potential *in vivo*.

Conflict of interest

The authors declare no conflict of interest.

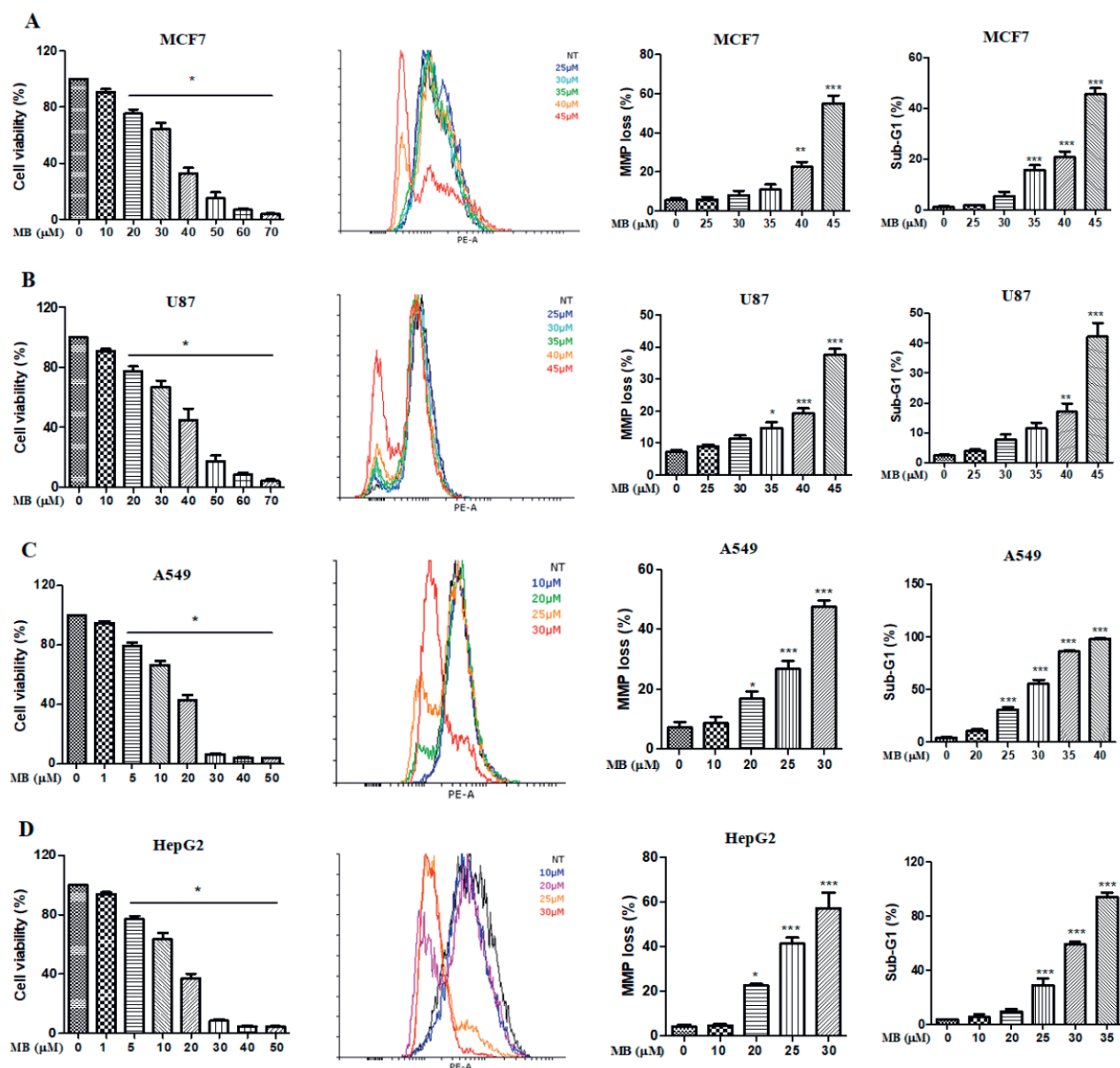


Fig. 8. MB decreased cell viability in various cancer cells. The cells were treated with the indicated concentrations of MB for 24 h, and cell viability was evaluated using the MTT assay. The fraction of cells with a low MMP (%) and sub-G1 phase accumulation was evaluated by flow cytometry. **A:** MCF7 cells, **B:** U87 cells, **C:** A549 cells, **D:** HepG2 cells. Overlay histogram representing MMP loss with the formation of left-side waves indicates loss of potential, compared with the right-side wave showing high potential in control and healthy cells. The Y-axis shows the number of cells. The X-axis shows the potential of the mitochondrial membrane. The data in each bar graph are presented as the means \pm SEM. (N = 3). * $P < 0.05$, ** $P < 0.01$ and *** $P < 0.001$ relative to control.

Author contributions

Yongchao Li and Mengling Li performed experiments, analysed data, prepared figures, and drafted the manuscript. Kanwal Ahmed drafted and edited the manuscript. Jing Yang and Linlin Song analysed part of the data and prepared figures. Loreto Feril analysed part of the data and edited the manuscript. Zheng-Guo Cui and Yusuke Hiraku contributed to this work by designing experiments, providing intellectual input, supervising

the research, and edited the manuscript. All authors reviewed and approved the manuscript for submission. Yongchao Li and Mengling Li contributed equally.

Acknowledgements

We genuinely appreciate Dr. Qing-Li Zhao and Dr. Ryohei Ogawa (Department of Radiological Sciences, Graduate School of Medicine and Pharmaceutical Sciences, University of Toyama, Japan) for their helpful discussions.

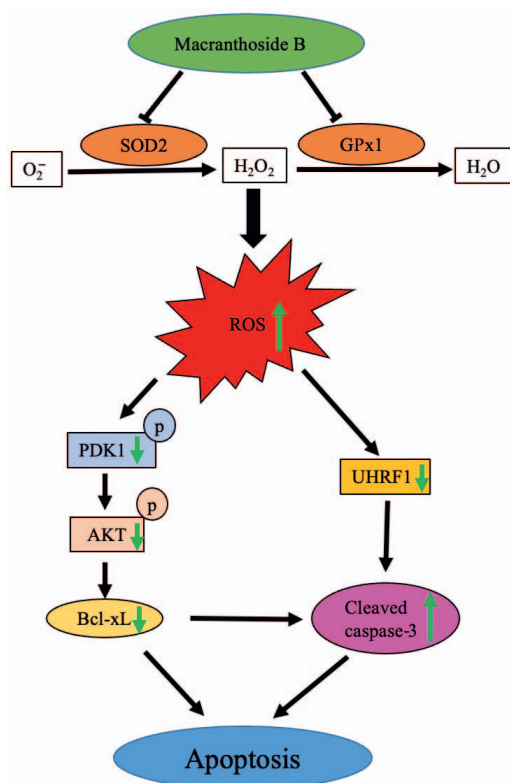


Fig. 9. Schematic summary of pathways involved in MB-induced apoptosis in HeLa cells.

References

- Avato, P., Migoni, D., Argentieri, M., Fanizzi, F. P., Tava, A. (2017) Activity of saponins from *Medicago* species against HeLa and MCF-7 cell lines and their capacity to potentiate cisplatin effect. *Anticancer Agents Med. Chem.* **17**, 1508-1518.
- Bagli, E., Stefanidou, M., Morbidelli, L., Ziche, M., Psillas, K., Murphy, C., Fotsis, T. (2004) Luteolin inhibits vascular endothelial growth factor-induced angiogenesis; inhibition of endothelial cell survival and proliferation by targeting phosphatidylinositol 3'-kinase activity. *Cancer Res.* **64**, 7936-7946.
- Bahrami, A., Hasanzadeh, M., Hassanian, S. M., ShahidSales, S., Ghayour-Mobarhan, M., Ferns, G. A., Avan, A. (2017) The potential value of the PI3K/Akt/mTOR signaling pathway for assessing prognosis in cervical cancer and as a target for therapy. *J. Cell. Biochem.* **118**, 4163-4169.
- Bhatla, N., Aoki, D., Sharma, D. N., Sankaranarayanan, R. (2018) Cancer of the cervix uteri. *Int. J. Gynaecol. Obstet.* **143**(Suppl 2), 22-36.
- Chen, C. Y., Qi, L. W., Yi, L., Li, P., Wen, X. D. (2009) Liquid chromatography-mass spectrometry analysis of macranthoside B, macranthoside A, dipsacoside B, and macranthoside B in rat plasma for the pharmacokinetic investigation. *J. Chromatogr. B, Analyt. Technol. Biomed. Life Sci.* **877**, 159-165.
- Chen, X., Zhou, Y. L., Liang, S. Y., Shi, Y. C., Lin, S., Shu, M. Q. (2019) Overexpression of UHRF1 promoted the proliferation of vascular smooth cells via the regulation of Geminin protein levels. *Biosci. Rep.* **39**, BSR20181341.
- Choi, J. H., Yang, Y. R., Lee, S. K., Kim, S. H., Kim, Y. H., Cha, J. Y., Oh, S. W., Ha, J. R., Ryu, S. H., Suh, P. G. (2008) Potential inhibition of PDK1/Akt signaling by phenothiazines suppresses cancer cell proliferation and survival. *Ann. N. Y. Acad. Sci.* **1138**, 393-403.
- Cragg, G. M., Newman, D. J. (2005) Plants as a source of anti-cancer agents. *J. Ethnopharmacol.* **100**, 72-79.
- Cui, Z. G., Kondo, T., Matsumoto, H. (2006) Enhancement of apoptosis by nitric oxide released from alpha-phenyl-tert-butyl nitron under hyperthermic conditions. *J. Cell. Physiol.* **206**, 468-476.
- Ferlay, J., Soerjomataram, I., Dikshit, R., Eser, S., Mathers, C., Rebelo, M., Parkin, D. M., Forman, D., Bray, F. (2015) Cancer incidence and mortality worldwide: sources, methods and major patterns in GLOBOCAN 2012. *Int. J. Cancer* **136**, E359-E386.
- Fonseca-Silva, F., Inacio, J. D., Canto-Cavaleiro, M. M., Almeida-Amaral, E. E. (2011) Reactive oxygen species production and mitochondrial dysfunction contribute to quercetin induced death in *Leishmania amazonensis*. *PLoS One* **6**, e14666.
- Guan, F., Shan, Y., Zhao, X., Zhang, D., Wang, M., Peng, F., Xia, B., Feng, X. (2011) Apoptosis and membrane permeabilisation induced by macranthoside B on HL-60 cells. *Nat. Prod. Res.* **25**, 332-340.
- Harris, T. K. (2003) PDK1 and PKB/Akt: ideal targets for development of new strategies to structure-based drug design. *IUBMB Life* **55**, 117-126.
- Jiang, P., Sheng, Y. C., Chen, Y. H., Ji, L. L., Wang, Z. T. (2014) Protection of *Flos Lonicerae* against acetaminophen-induced liver injury and its mechanism. *Environ. Toxicol. Pharmacol.* **38**, 991-999.
- Johnson-Cadwell, L. I., Jekabsons, M. B., Wang, A., Polster, B. M., Nicholls, D. G. (2007) 'Mild Uncoupling' does not decrease mitochondrial superoxide levels in cultured cerebellar granule neurons but decreases spare respiratory capacity and increases toxicity to glutamate and oxidative stress. *J. Neurochem.* **101**, 1619-1631.
- Joshi, P., Vishwakarma, R. A., Bharate, S. B. (2017) Natural alkaloids as P-gp inhibitors for multidrug resistance reversal in cancer. *Eur. J. Med. Chem.* **138**, 273-292.
- Kharbanda, S., Pandey, P., Schofield, L., Israels, S., Roncinske, R., Yoshida, K., Bharti, A., Yuan, Z. M., Saxena, S., Weichselbaum, R., Nalin, C., Kufe, D. (1997) Role for Bcl-xL as an inhibitor of cytosolic cytochrome C accumulation in DNA damage-induced apoptosis. *Proc. Natl. Acad. Sci. USA* **94**, 6939-6942.
- Lazorchak, A. S., Su, B. (2011) Perspectives on the role of mTORC2 in B lymphocyte development, immunity and tumorigenesis. *Protein Cell* **2**, 523-530.
- Li, M., Cui, Z. G., Zakki, S. A., Feng, Q., Sun, L., Feril, L. B. Jr., Inadera, H. (2019) Aluminum chloride causes 5-fluorouracil resistance in hepatocellular carcinoma HepG2 cells. *J. Cell. Physiol.* **234**, 20249-20265.
- Li, X. L., Meng, Q. H., Fan, S. J. (2009) Adenovirus-mediated expression of UHRF1 reduces the radiosensitivity of cervical cancer HeLa cells to γ -irradiation. *Acta Pharmacol. Sin.* **30**, 458-466.

- Liu, P., Cheng, H., Roberts, T. M., Zhao, J. J. (2009) Targeting the phosphoinositide 3-kinase pathway in cancer. *Nat. Rev. Drug. Discov.* **8**, 627-644.
- Majumder, D., Das, A., Saha, C. (2017) Catalase inhibition an anti cancer property of flavonoids: a kinetic and structural evaluation. *Int. J. Biol. Macromol.* **104**, 929-935.
- Nitulescu, G. M., Margina, D., Juzenas, P., Peng, Q., Oлару, O. T., Saloustros, E., Fenga, C., Spandidos, D., Libra, M., Tsatsakis, A. M. (2016) Akt inhibitors in cancer treatment: the long journey from drug discovery to clinical use (review). *Int. J. Oncol.* **48**, 869-885.
- Nitulescu, G. M., Van De Venter, M., Nitulescu, G., Unguriaanu, A., Juzenas, P., Peng, Q., Oлару, O. T., Gradinaru, D., Tsatsakis, A., Tsoukalas, D., Spandidos, D. A., Margina, D. (2018) The Akt pathway in oncology therapy and beyond (review). *Int. J. Oncol.* **53**, 2319-2331.
- Ohta, S., Sato, N., Tu, S. H., Shinoda, M. (1993) Protective effects of Taiwan crude drugs on experimental liver injuries. *Yakugaku Zasshi* **113**, 870-880. (in Japanese)
- Prasad, S. B., Yadav, S. S., Das, M., Modi, A., Kumari, S., Pandey, L. K., Singh, S., Pradhan, S., Narayan, G. (2015) PI3K/AKT pathway-mediated regulation of p27(Kip1) is associated with cell cycle arrest and apoptosis in cervical cancer. *Cell. Oncol. (Dordr.)* **38**, 215-225.
- Prasedya, E. S., Miyake, M., Kobayashi, D., Hazama, A. (2016) Carrageenan delays cell cycle progression in human cancer cells in vitro demonstrated by FUCCI imaging. *BMC Complement. Altern. Med.* **16**, 270.
- Redza-Dutordoir, M., Averill-Bates, D. A. (2016) Activation of apoptosis signalling pathways by reactive oxygen species. *Biochim. Biophys. Acta* **1863**, 2977-2992.
- Riccardi, C., Nicoletti, I. (2006) Analysis of apoptosis by propidium iodide staining and flow cytometry. *Nat. Protoc.* **1**, 1458-1461.
- Sambrook, J., Fritsch, T., Maniatis, T. (1989) *Molecular Cloning: A Laboratory Manual. 1*. Cold Spring Harbor Laboratory Press, New York.
- Shan, Y., Guan, F., Zhao, X., Wang, M., Chen, Y., Wang, Q., Feng, X. (2016) Macranthoside B induces apoptosis and autophagy via reactive oxygen species accumulation in human ovarian cancer A2780 cells. *Nutr. Cancer* **68**, 280-289.
- Stevens, M., Oltean, S. (2019) Modulation of the apoptosis gene Bcl-x function through alternative splicing. *Front. Genet.* **10**, 804.
- Sun, L., Zhang, Q., Luan, H., Zhan, Z., Wang, C., Sun, B. (2011) Comparison of KRAS and EGFR gene status between primary non-small cell lung cancer and local lymph node metastases: implications for clinical practice. *J. Exp. Clin. Cancer Res.* **30**, 30.
- Wang, J., Zhao, X. Z., Qi, Q., Tao, L., Zhao, Q., Mu, R., Gu, H. Y., Wang, M., Feng, X., Guo, Q. L. (2009) Macranthoside B, a hederagenin saponin extracted from *Lonicera macranthoides* and its anti-tumor activities in vitro and in vivo. *Food Chem. Toxicol.* **47**, 1716-1721.
- Wang, Y., Yuan, Y., Gao, Y., Li, X., Tian, F., Liu, F., Du, R., Li, P., Wang, F., Xu, S., Wu, X., Wang, C. (2019) MicroRNA-31 regulating apoptosis by mediating the phosphatidylinositol-3 kinase/protein kinase B signaling pathway in treatment of spinal cord injury. *Brain Dev.* **41**, 649-661.
- Webster, K. A. (2012) Mitochondrial membrane permeabilization and cell death during myocardial infarction: roles of calcium and reactive oxygen species. *Future Cardiol.* **8**, 863-884.
- Yun, S. M., Woo, S. H., Oh, S. T., Hong, S. E., Choe, T. B., Ye, S. K., Kim, E. K., Seong, M. K., Kim, H. A., Noh, W. C., Lee, J. K., Jin, H. O., Lee, Y. H., Park, I. C. (2016) Melatonin enhances arsenic trioxide-induced cell death via sustained upregulation of Redd1 expression in breast cancer cells. *Mol. Cell. Endocrinol.* **422**, 64-73.
- Zakki, S. A., Cui, Z. G., Sun, L., Feng, Q. W., Li, M. L., Inadera, H. (2018) Baicalin augments hyperthermia-induced apoptosis in U937 cells and modulates the MAPK pathway via ROS generation. *Cell. Physiol. Biochem.* **45**, 2444-2460.